Intense narrow band terahertz generation via type-II difference-frequency generation in ZnTe using chirped optical pulses

J. R. Danielson,[1] A. D. Jameson,[1] J. L. Tomaino,[1] H. Hui,[1] J. D. Wetzel,[1] Yun-Shik Lee,[1,a)] and K. L. Vodopyanov[2]
[1]*Department of Physics, Oregon State University, Corvallis, Oregon 97331-6507, USA*
[2]*E. L. Ginzton Laboratory, Stanford University, Stanford, California 94305, USA*

(Received 27 January 2008; accepted 29 May 2008; published online 11 August 2008)

We developed a tabletop source of intense, narrow band terahertz pulses via type-II difference-frequency generation in ZnTe crystal using two linearly chirped and orthogonally polarized optical pulses. The pulse energy is in the range of 1–3 nJ depending on the variable pulse duration from 1 to 5 ps. The amplitude of electric field reaches ~10 kV/cm. The central frequency of the spectrum is continuously tunable from 0.3 to 2.5 THz with the bandwidth at 0.2–0.5 THz.
 [DOI: 10.1063/1.2959846]

Bright, tunable sources of narrow band terahertz radiation are in great demand for a wide range of scientific and technological applications. An exciting yet uncharted regime of terahertz research activities is the nonlinear interactions of terahertz radiation with physical, chemical, and biological media, which can drive material systems into dynamic states in thermal nonequilibrium. The nonlinear interactions involve low-energy excitations that correspond to terahertz frequencies. Some elementary excitons of cardinal interest include Rydberg transitions in atoms,[1,2] transitions among impurity states in semiconductors,[3] intraband transitions in semiconductor nanostructures,[4,5] many-body interactions in strongly correlated electron systems,[6] phonon modes in organic and inorganic crystals,[7] rotational transitions in molecules,[8] and collective large-amplitude motions in biological molecules.[9]

Free electron lasers (FELs) are outstanding sources of strong and narrow band terahertz radiation. Many important scientific and technical achievements have capitalized on the favorable characteristics of FELs such as high power and broad tunability. An example is the coherent manipulation of quantum states in semiconductors capacitated by the intense terahertz radiation of FELs.[3–5] FELs, however, have an accessibility issue. All FELs are operated as user facilities because of their size and cost. Alternatively, molecular gas lasers pumped by CO_2 lasers are powerful, tabletop sources of continuous-wave (cw) terahertz radiation.[10] A critical drawback of the gas lasers is their lack of tunability. Their operational frequencies are determined by specific molecular transitions.

A few tabletop sources have been developed to generate tunable, narrow band terahertz pulses using broadband optical pulses: mixing chirped optical pulses in a photoconductive (PC) antenna,[11] optical rectification of shaped pulses,[12] and optical rectification in quasiphase matching nonlinear crystals.[13] In addition to the relative compactness and continuous tunability, another advantage of these ultrafast optical methods is noteworthy: They can be utilized to carry out time-resolved studies on terahertz-induced nonlinear effects with a subpicosecond resolution only limited by the transform-limited optical pulse duration. Although the output intensities of the previous works were too weak to attain any of the terahertz nonlinear effects mentioned above, their potential has not been fully explored yet. A glimpse of the potential has been shown in the recent time-resolved study on interaction of strong single-cycle terahertz pulses with semiconductor quantum wells, where the nonlinear effects were so strong that the normalized differential transmission of the exciton lines induced by terahertz pulses reached up to 60%.[14]

In this work, we demonstrate the generation of intense, narrow band terahertz pulses using an experimental scheme, a modification to the method of mixing two colinearly polarized and linearly chirped optical pulses in a PC antenna.[11] We utilize an electro-optical crystal, 1 mm ZnTe instead of a PC antenna. The applied optical pulse energy is ~1 mJ so that PC antennas are either incapable of sustaining the high peak power or inefficient because of the saturation arising from finite capacitance. Furthermore, the efficiency of PC switching drops rapidly above ~1 THz due to the finite carrier relaxation time (~0.5 ps) of the substrate materials. We cross polarize the two optical pump pulses with two advantages over the case of two parallel pump polarizations: First, cross-polarized beams can be recombined without any loss in power (in contrast, no optical arrangement can salvage more than half of input power while combining two beams with parallel polarizations). Second, employing type-II difference-frequency generation (DFG) can reduce parasitic nonlinear effects such as free-carrier generation induced by multiphoton absorption. We will discuss our experimental scheme in detail in Sec. II.

I. TYPE-II DFG IN ZINC TELLURIDE USING LINEARLY CHIRPED OPTICAL PULSES

The crystal class of ZnTe is $\bar{4}3m$, thus its second-order nonlinear susceptibility tensor has six nonvanishing elements, and only one is independent,

a)Electronic mail: leeys@physics.oregonstate.edu.

$$2d_{14} \equiv \chi^{(2)}_{xyz} = \chi^{(2)}_{xzy} = \chi^{(2)}_{yzx} = \chi^{(2)}_{yxz} = \chi^{(2)}_{zxy} = \chi^{(2)}_{zyx}. \quad (1)$$

Given the two orthogonally polarized optical pump fields,

$$\mathbf{E}_1(\omega_1) = \mathbf{E}_1 e^{-i\omega_1 t} \quad \text{and} \quad \mathbf{E}_2(\omega_2) = \mathbf{E}_2 e^{-i\omega_2 t}, \quad (2)$$

incident normally on a ⟨110⟩ ZnTe crystal, the second-order nonlinear polarization of type-II DFG is expressed as

$$\mathbf{P}^{(2)}(\omega_3) = 2\epsilon_0 d_{14} E_1 E_2^* e^{-i\omega_3 t} \begin{pmatrix} -\sqrt{2}\cos 2\phi \\ \sqrt{2}\cos 2\phi \\ \sin 2\phi \end{pmatrix}, \quad (3)$$

where $\omega_3 (= \omega_1 - \omega_2)$ is the difference frequency and ϕ is the angle between $\mathbf{E}_1$ and the $[1\bar{1}0]$ axis. The maximum DFG is obtained when the optical fields are polarized along the $[1\bar{1}0]$ and [001] axes, respectively, i.e., $\phi = 0$ or $\pi/2$. In this arrangement, the DFG polarization is parallel to the $[1\bar{1}0]$ axis.

When two identical Gaussian pulses are linearly chirped and separated by a relative time delay τ, the fields are written as

$$E_1(t) = E_2(t+\tau) = E_0 e^{-at^2} e^{-i(\omega + bt)t}, \quad (4)$$

where ω is the central frequency, $\tau_p = \sqrt{2 \ln 2/a}$ is the pulse duration, and b is the chirp parameter. The instantaneous frequencies are given by

$$\omega_1 = \omega + 2bt \quad \text{and} \quad \omega_2 = \omega + 2b(t-\tau), \quad (5)$$

which leads to the difference frequency,

$$\omega_3 = 2\pi\nu_3 = 2b\tau, \quad (6)$$

depending on the time delay and the chirp parameter. The difference frequency is independent of time, i.e., if the two pulses are mixed in a ZnTe crystal, the DFG polarization oscillates at the same frequency throughout the interaction of the two pulses.

II. EXPERIMENTAL ARRANGEMENT

The optical source was 1 kHz Ti:sapphire regenerative amplifier (Legend, Coherent, Inc.) with 1 mJ pulse energy. We introduced a linear chirp by adjusting the grating space in the output compressor of the amplifier. The pulse duration was continuously tunable from 0.1 to 4.6 ps. The duration of the driving optical pulse was measured using an intensity autocorrelator assuming a Gaussian pulse envelope.

The optical beam was divided and recombined in an apparatus, as shown in Fig. 1(a). The input beam was *s*-polarized and split with a 50/50 beam splitter (BS). One path was sent through a quarter-wave plate twice that rotated the polarization by 90°. The path length of this beam was adjusted to introduce a relative time delay. A thin film polarizer (TFP) recombined these two beams, transmitting *s*-polarization and reflecting *p*-polarization. The output of the arrangement was two orthogonally polarized pulses with a relative time delay. They were sent through a 1 mm ⟨110⟩ ZnTe crystal, with the polarizations aligned to the $[1\bar{1}0]$ and [001] axes to generate terahertz radiation using type-II DFG. The spot size on the crystal was measured as ~3 mm.

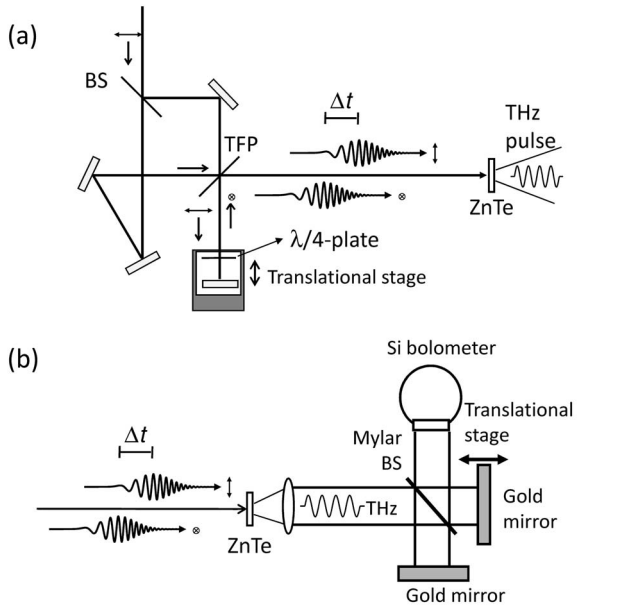

FIG. 1. Schematics of the experimental setup for generation of tunable narrow band terahertz pulses. (a) Taking a linearly chirped optical pulse, the optical arrangement produces two orthogonally polarized pulses with a time delay. The BS separates the beam; a double pass through the λ/4 wave plate in one path rotates the beam polarization by 90°; the translational stage gives the time delay; the TFP combines the two beams. The two pulses generate a narrow band terahertz pulse using type-II DFG in a 1 mm ZnTe crystal. The terahertz output power is measured using a Si bolometer. (b) The terahertz Michelson interferometer is utilized to determine terahertz power spectra by measuring interferometric autocorrelations.

There is a significant advantage in this arrangement over a Michelson interferometer, as almost all input power is transmitted through the device. We measured 90% energy transmission with losses due largely to the small size of our TFP clipping the beam edges. Another advantage is that parasitic nonlinear effects are minimized along the [001] axis. We are in the regime that terahertz output power is saturated because of unwanted nonlinear processes such as two-photon absorption and consequent free carriers. For a zinc-blende crystal, nonlinear absorption is anisotropic and tends to minimize with optical polarization parallel to the ⟨100⟩ axis and maximum to the ⟨111⟩ axis.[15]

We used a silicon bolometer to measure the terahertz radiation power. Calibrating the bolometer, we took into account the pulsed nature of our source. We applied a detector responsivity of 9.26×10^9 V/J or 9.26×10^6 V/W with 1 kHz repetition rate. This is about one-tenth of the responsivity calibrated with cw sources.

To measure the spectra of the emitted radiation, we built a terahertz Michelson interferometer using a Mylar BS and performed field autocorrelations. This arrangement is shown in Fig. 1(b). While this method loses the phase information of the spectrum, it allows to extract, via Fourier transform, the power spectrum of the pulse.

III. MEASUREMENTS

Figure 2 shows a typical terahertz field autocorrelation and associated spectrum when the optical pulse duration and the time delay are 4.11 and 1.90 ps, respectively. The tera-

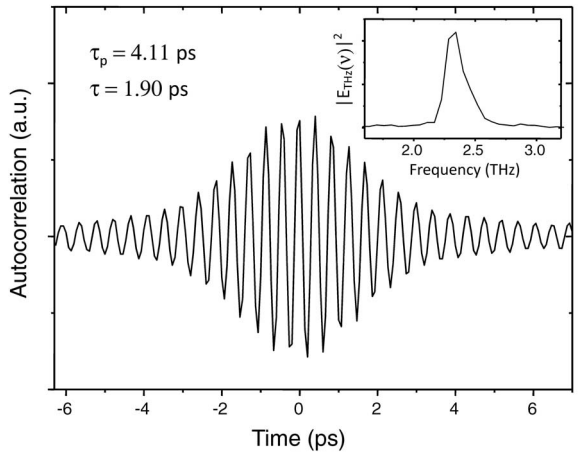

FIG. 2. (a) A field autocorrelation of the generated terahertz radiation. The optical pulse duration and the time delay are 4.11 and 1.90 ps, respectively. Its corresponding spectrum is shown in the inset.

hertz radiation is narrow band; the spectrum centered at 2.34 terahertz has a spectral width of ~0.2 THz with an associated quality factor of ~11.

The experimental setup is capable of fine and continuous frequency tuning. Figure 3 shows a set of spectra of the terahertz radiation with central frequencies ranging from 1.8 to 2.5 THz. The water absorption lines near 2.2 THz are visible. For this measurement, the optical pulse duration is held constant at 4.11 ps, and the time delay between the two pulses varies from 1.50 to 2.03 ps. The frequency of the terahertz radiation varies linearly with pulse delay, as shown in the inset of Fig. 3. The solid line is the best linear fit to the data, which leads to the chirp parameter $b=3.85\ \mathrm{ps}^{-2}$ using $\nu_3=(b/\pi)\tau$ from Eq. (6). Figure 4 shows the emitted terahertz power as a function of frequency adjusted by the delay time for a variety of optical pulse durations, $\tau_p=1.06$, 2.13, 2.78, 3.35, and 4.61 ps. As the pulse duration is increased, the peak power of the terahertz radiation is reduced: 3 μW for $\tau_p=1.06$ ps and 1 μW for $\tau_p=4.61$ ps. For pulses

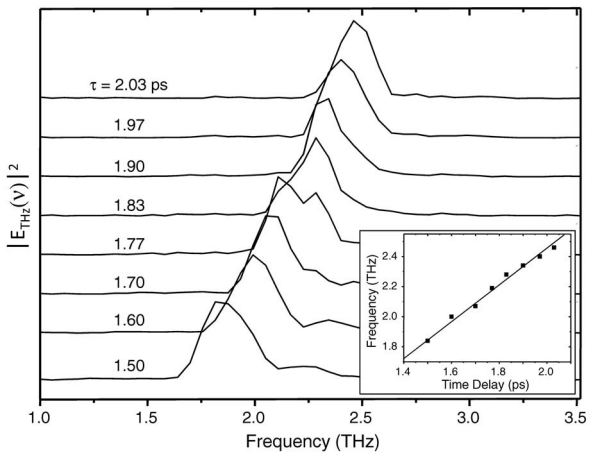

FIG. 3. The spectra for terahertz radiation driven by two optical pulses of duration 4.11 ps when the relative time delays between them are 1.50, 1.60, 1.70, 1.77, 1.83, 1.90, 1.97, and 2.00 ps. The inset shows the central frequencies of the spectra as a function of pulse delay. The solid line fits the data.

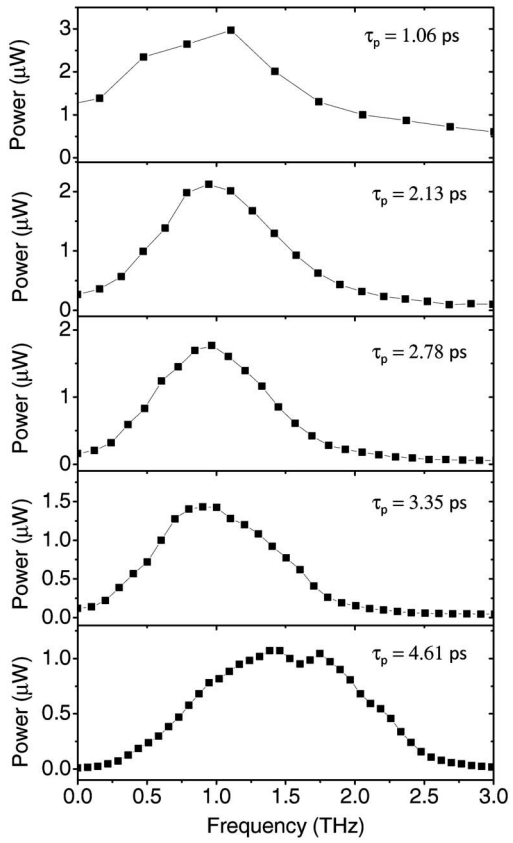

FIG. 4. Emitted terahertz beam power as a function of central frequency for the pulses of duration $\tau_p=1.06$, 2.13, 2.78, 3.35, and 4.61 ps.

shorter than 3.35 ps, the maximum power is obtained near 1 THz and the bandwidth is ~1 THz. The longest pulses ($\tau_p=4.61$ ps) produce the maximum terahertz power around 1.5 THz, and the bandwidth is ~1.5 THz. The data shows two dips at 1.7 and 2.2 THz corresponding to water absorption lines.

The spectral profile of the radiation power is mainly determined by two factors: First, the radiation field is a quadratic function of frequency, which accounts for low radiation power at low frequencies. Second, as we tune the frequency by adjusting the time delay, the two optical pulses overlap less and less in time as the frequency increases, and so for larger frequencies the terahertz radiation power also falls away.

For the 1.06 ps pulse duration the terahertz power does not vanish either at low or high frequencies because the relatively short pulses produce additional terahertz radiation using optical rectification. The process involves only the pulses with the polarization parallel to $[1\bar{1}0]$. Optical rectification gives a broadband terahertz emission and is easily distinguished from the type-II DFG emission since it has a different angular dependence as the ZnTe crystal is rotated.

Figure 5 shows the terahertz radiation power as a function of time delay. In this case, the range is extended to negative time delays, where the pulse with polarization parallel to the $[1\bar{1}0]$ axis—designated as pulse 1—precedes the other, pulse 2. The data show a notable imbalance in the

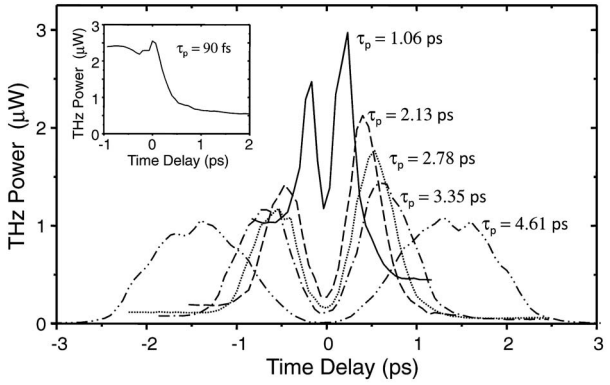

FIG. 5. Emitted terahertz power for both negative and positive delays. Inset shows optical rectification signal for negative and positive delays.

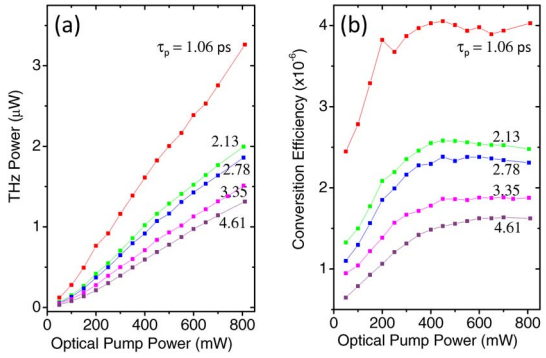

FIG. 6. (Color online) (a) terahertz power curve as a function of input power. (b) terahertz conversion efficiency as a function of input power.

emission for negative time delays, which can be accounted for by the anisotropy of the nonlinear absorption processes.

The inset of Fig. 5 is useful in understanding this asymmetry. It shows the terahertz emission power for fully compressed 90 fs pulses. In this case the whole emission is generated by optical rectification. The pulse is still sent through the splitter, so the driving pulse incident on the ZnTe crystal is two orthogonally polarized pulses, one leading the other. In this arrangement, only pulse 1 contributes to the terahertz generation using optical rectification. For positive time delays, the pulse 1 and the Terahertz pulse are absorbed by free carriers generated by the preceding pulse 2 through parasitic nonlinear effects, thus the Terahertz power is lower than that for negative time delays, where the pulse 2 has no effect. The effect diminishes as the pulse duration increases; it is still pronounced for 1.06 ps data, visible for 2.13, 2.78, and 3.35 ps data, and negligible for 4.61 ps data.

The terahertz power of DFG shows an opposite trend: The efficiency of terahertz generation is higher for positive time delays. The reason is as follows: Eventually, pulse 1 exerts stronger parasitic nonlinear effects than pulse 2.[15] Therefore, the terahertz radiation using DFG, involving both pulses 1 and 2, sees less of the parasitic effects for a positive time than the other way around. For the longest pulse duration of 4.61 ps, this asymmetry disappears.

Finally, Fig. 6 shows the terahertz radiation power as a function of input optical power and the optical-to-terahertz conversion efficiency curves. We see that in the range of powers we used, the emitted power reached a saturated value. Below a certain value of pump, with an average intensity of 3.8 W/cm^2, the terahertz power varies quadratically with the input power, as expected for a second-order process. Above this pump level it varies almost linearly with input power. The saturation of the conversion efficiency can be attributed to the parasitic nonlinear effects in the ZnTe crystal.

IV. CONCLUSION

We have demonstrated an experimental scheme for generating strong, narrow band, and tunable terahertz radiation. This arrangement is advantageous over previous incarnations because (i) no pump power is wasted in the pulse splitting device and (ii) the terahertz generation mechanism is type-II DFG, allowing less parasitic nonlinear effects comparing with type-I DFG. This tabletop source is relatively simple and compact, and can be integrated easily into an ultrafast spectroscopy setup.

[1]N. E. Tielking and R. R. Jones, Phys. Rev. A **52**, 1371 (1995).
[2]J. Ahn, D. N. Hutchinson, C. Rangan, and P. H. Bucksbaum, Phys. Rev. Lett. **86**, 1179 (2001).
[3]B. E. Cole, J. B. Williams, B. T. King, M. S. Sherwin, and C. R. Stanley, Nature (London) **410**, 60 (2001).
[4]K. B. Nordstrom, K. Johnsen, S. J. Allen, A.-P. Jauho, B. Birnir, J. Kono, T. Noda, H. Akiyama, and H. Sakaki, Phys. Rev. Lett. **81**, 457 (1998).
[5]S. G. Carter, V. Birkedal, C. S. Wang, L. A. Coldren, A. V. Maslov, D. S. Citrin, and M. S. Sherwin, Science **310**, 651 (2005).
[6]N. Kida, H. Murakami, and M. Tonouchi, in *Terahertz Optoelectronics*, edited by K. Sakai (Springer-Verlag, Berlin, 2005), Chap. 6, pp. 275–334.
[7]M. Schall, M. Walther, and P. Uhd Jepsen, Phys. Rev. B **64**, 094301 (2001).
[8]H. Harde, S. Keiding, and D. Grischkowsky, Phys. Rev. Lett. **66**, 1834 (1991).
[9]T. R. Globus, D. L. Woolard, T. Khromova, T. W. Crowe, M. Bykhovskaia, B. L. Gelmont, J. Hesler, and A. C. Samuels, J. Biol. Phys. **29**, 89 (2003).
[10]F. K. Kneubühl, D. P. Scherrer, and D. B. Moix, Arch. Elektrotech. (Berlin) **77**, 35 (1993).
[11]A. S. Weling and D. H. Auston, J. Opt. Soc. Am. B **13**, 2783 (1996).
[12]J. Ahn, A. Efimov, R. Averitt, and A. Taylor, Opt. Express **11**, 2486 (2003).
[13]Y. -S. Lee, T. Meade, T. B. Norris, and A. Galvanaukas, Appl. Phys. Lett. **78**, 3583 (2001).
[14]J. R. Danielson, Yun-Shik Lee, J. P. Prineas, J. T. Steiner, M. Kira, and S. W. Koch, Phys. Rev. Lett. **99**, 237401 (2007).
[15]W. C. Hurlbut, Yun-Shik Lee, K. L. Vodopyanov, P. S. Kuo, and M. M. Fejer, Opt. Lett. **32**, 668 (2007).